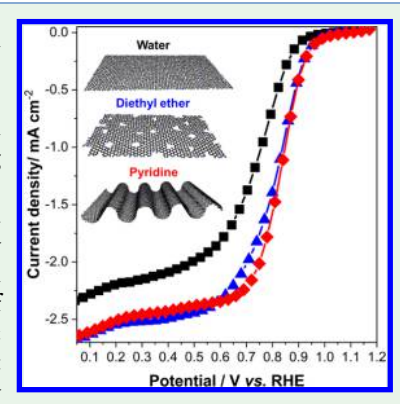
www.acsanm.org

Nitrogen-Doped Graphene Oxide Electrocatalysts for the Oxygen **Reduction Reaction**

Joseph H. Dumont, †, † Ulises Martinez, † Kateryna Artyushkova, † Geraldine M. Purdy, † Andrew M. Dattelbaum, † Piotr Zelenay, † Aditya Mohite, † Plamen Atanassov, † and Gautam Gupta*, †

Supporting Information

ABSTRACT: Platinum group metal-free (PGM-free) electrocatalysts for the oxygen reduction reaction (ORR) often exhibit a complex functionalized graphitic structure. Because of this complex structure, limited understanding exists about the design factors for the synthesis of high-performing materials. Graphene, a two-dimensional hexagonal structure of carbon, is amenable to structural and functional group modifications, making it an ideal analogue to study crucial properties of more complex graphitic materials utilized as electrocatalysts. In this paper, we report the synthesis of active nitrogen-doped graphene oxide catalysts for the ORR in which their activity and four-electron selectivity are enhanced using simple solvent and electrochemical treatments. The solvents, chosen based on Hansen's solubility parameters, drive a substantial change in the morphology of the functionalized graphene materials by (i) forming microporous holes in the graphitic sheets that lead to edge defects and (ii) inducing 3D structure in the graphitic sheets that promotes ORR. Additionally, the cycling of these catalysts has highlighted the multiplicity of the active sites, with different durability, leading to a highly selective catalyst over time,



with a minimal loss in performance. High ORR activity was demonstrated in an alkaline electrolyte with an onset potential of ~1.1 V and half-wave potential of 0.84 V vs RHE. Furthermore, long-term stability potential cycling showed minimal loss in half-wave potential (<3%) in both N₂- and O₂-saturated solutions with improved selectivity toward the four-electron reduction after 10000 cycles. The results described in this work provide additional understanding about graphitic electrocatalysts in alkaline media that may be utilized to further enhance the performance of PGM-free ORR electrocatalysts.

KEYWORDS: oxygen reduction reaction, active sites, graphene, graphene oxide, alkaline

evelopment of novel electrocatalysts for the oxygen reduction reaction (ORR) is crucial for numerous electrochemical energy conversion and storage devices such as metal-air batteries, fuel cells, and certain electrolyzers. 1-4 Fuel cells, in particular, rely on costly and scarce platinum group metal (PGM) catalysts for ORR, 5,6 thus stimulating efforts to develop PGM-free catalysts. Recently developed PGM-free catalysts synthesized from earth-abundant elements, e.g., carbon, nitrogen, and iron, have shown promising ORR activity in alkaline electrolyte and have the potential to significantly impact several commercial applications.^{7,8} In alkaline environments, the ORR can proceed via a 4- or 2 + 2-electron pathway according to the following reactions:

$$O_2 + 2H_2O + 4e^- \rightarrow 4OH^-$$
 (1)

$$O_2 + H_2O + 2e^- \rightarrow HO_2^- + OH^-$$
 (2)

$$HO_2^- + H_2O + 2e^- \rightarrow 3OH^-$$
 (3)

The direct four-electron reduction pathway is described by eq 1. Alternatively, O2 can be reduced via a two-electron reaction as shown in eq 2 producing the hydroperoxyl radicals HO₂-, which are undesired as they are known to negatively affect membrane durability. 9-11 Additionally, in thicker electrode structures, the slow diffusion of products can further reduce HO₂⁻ to OH⁻ according to eq 3. However, a thicker electrode layer will consequently increase the mass transport barrier and the impedance of the electrode which are both detrimental to the electrochemical device such as the fuel cell. 12 Therefore, it is imperative to study the selectivity of the catalysts toward the ORR to develop highly selective PGM-free catalysts for maximizing the four-electron reaction and for eliminating the production of harmful radicals and the need for thicker electrodes.

The best performing PGM-free electrocatalysts have traditionally been synthesized from the pyrolysis of transition metal precursors, nitrogen-containing compounds, and porous carbons supports producing complex N-doped graphitic structures. 13-25 However, there is currently limited understanding of the design parameters that can allow for tailored synthesis of PGM-free catalytic materials. Furthermore, the

Received: January 21, 2019 Accepted: February 1, 2019 Published: February 1, 2019



[†]Los Alamos National Laboratory, Los Alamos, New Mexico 87545, United States

[‡]University of New Mexico, Albuquerque, New Mexico 87131, United States

origin of selectivity for ORR from these highly heterogeneous carbon structures has not been studied, which limits the understanding of the active site formation.^{7,26–30} Graphene, a two-dimensional hexagonal lattice of carbon, is amenable to structural and functional group modifications, 31-34 making it an ideal model structure that can be used to perform systematic investigations on catalyst formation. Importantly, the relatively simple graphene-based materials can be easily studied using spectroscopic techniques, such as Raman spectroscopy and X-ray photoelectron spectroscopy (XPS), to better understand the changes undergoing between the catalyst precursor form and the final catalyst material.³⁵ Functionalized graphene has already been shown to be ORRactive. 36-43 The conventional approach to synthesize resilient nitrogen-doped graphitic catalysts involves the exfoliation and functionalization of graphite using strong oxidizing agents. 32,34 which facilitate nitrogen incorporation via a high-temperature treatment in an ammonia-gas environment.³⁶ These nitrogendoped graphitic systems often produce lower ORR activity and selectivity than conventional nitrogen-doped mesoporous PGM-free catalysts. 36,43-46 This behavior is most likely due to a number of factors, namely fewer number of accessible active sites due to the restacking of N-doped graphitic sheets, limiting the diffusion of reactants. Recent studies have shown that multitudinous active sites contribute comparatively to the activity for oxygen reduction to peroxide and/or to water as well as peroxide electroreduction to water and nonelectrochemical disproportionation to peroxide.⁴⁷ Analysis of the individual contributions of heterogeneous active sites in advanced PGM-free catalysts is obscured by the fact that iron moieties atomically dispersed, associated with nitrogen, or displayed as nanoparticles of metallic iron or iron carbide contribute substantially to all these processes. 48,49 The role of the nitrogen moieties was targeted in recent studies,5 revealing that it has both independent contributions to hydrogen peroxide production and cocatalysis function of atomically dispersed iron. Making model catalysts by methods that specifically exclude any presence of iron becomes critical to understand the role of oxygen and nitrogen moieties and the contribution of carbonaceous matrix morphology through the contribution of one or more active sites to both activity and selectivity of oxygen reduction.

Here we describe the development of highly selective nitrogen-doped graphene-based model catalyst, structurally well-defined and modified via simple and controlled techniques that provide activity and functionality. This work advances the comprehension of PGM-free catalyst synthesis through the improvement of activity and selectivity using a combination of solvent and electrochemical treatments. The solvent treatment of graphene oxide results in drastic change in morphology of the catalytic materials that enhances its resulting ORR activity. Furthermore, cycling the catalyst further improves its selectivity. XPS and Raman spectroscopy were used to monitor the chemical changes of the functionalized graphene materials providing a strong correlation between structure and catalytic activity/selectivity. We observed an onset potential of ~1.1 V and half-wave potential of 0.84 V in alkaline media. Furthermore, long-term potential cycling resulted in only a minimal loss in half-wave potential in both N2- and O2saturated solutions, with improved selectivity toward the fourelectron reduction after 10000 cycles. This study brings light to the ORR performance of highly graphitic PGM-free catalysts and, more precisely, to the multiplicity of active sites and their

different stability and selectivity toward the ORR in alkaline medium.

The solvent-treatment process that we have developed to promote the four-electron ORR process on N-doped graphitic electrocatalysts in alkaline media is shown in Figure 1.

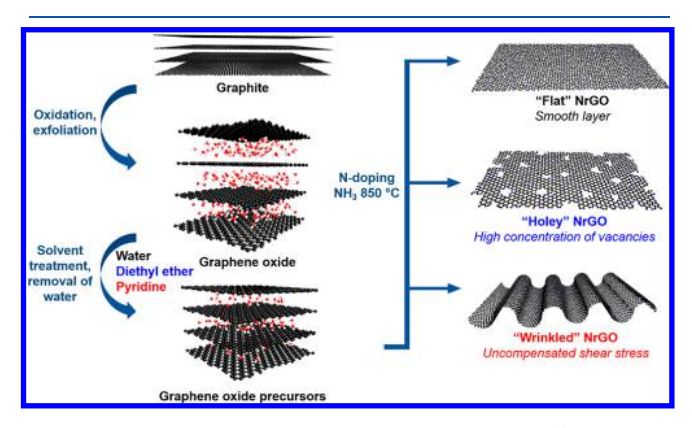


Figure 1. Schematic of synthesis process. Graphite is (i) exfoliated and oxidized into graphene oxide, (ii) treated with different solvents, and dried before (iii) nitrogen doping in a reactive ammonia atmosphere at high temperature (850 $^{\circ}$ C). The resulting morphology of the final catalyst is dependent on the solvent used to treat the graphene oxide prior to nitrogen doping.

Graphite, a compact stack of sp²-hybridized carbon sheets with an interplanar distance of 3.4 Å, is oxidized via a modified Hummers method, 31,34 forming oxygen-functionalized graphene, or graphene oxide (GO). The resulting GO nanosheets suspended in water are then exposed to different solvents. Structurally, the solvents utilized for this study are divided into two groups: noncyclic—water, ethanol, and diethyl ether—and cyclic—pyridine and toluene. Solvent structures and solubility properties are summarized in Figure S1. It is important to note that although organic solvents have been used to disperse GO,^{51,52} their effect on structure and properties has not been completely explored.⁴³ Critical solvent properties investigated here include Hansen's solubility parameters (dispersion, δ_d , hydrogen bonding, δ_{H} , and polarity, δ_{p}), water miscibility, and boiling point. These properties are important to consider because the GO nanosheets are predominantly solvated by H₂O molecules, which may affect the interaction between GO and other solvents. The dispersion parameter for all solvents studied is similar; however, their hydrogen bonding and polarity parameters vary significantly. Moreover, the miscibility of each solvent in water also varies; for example, while ethanol and pyridine are miscible in water, diethyl ether and toluene are only negligibly miscible. Because of varying solvent properties, vacuum-dried, solvent-treated GO, and untreated GO nanosheets displayed different interplanar distances (Figure S2). These solvent-treated GO nanosheets were then subjected to a high-temperature ammonia treatment (850 °C), resulting in nitrogen-doped reduced-graphene oxide (NrGO) electrocatalysts.

Structural and functional characterization of NrGO electrocatalysts was performed using a number of different techniques including X-ray diffraction (XRD), XPS, Raman spectroscopy, and scanning electron microscopy (SEM). Both XRD (Figure S2) and XPS (Figure 2a—c and Figure S3) characterization techniques revealed only minor differences in the structure and elemental speciation of all solvent-treated NrGO electrocatalysts. XRD patterns indicate minimal differences in the

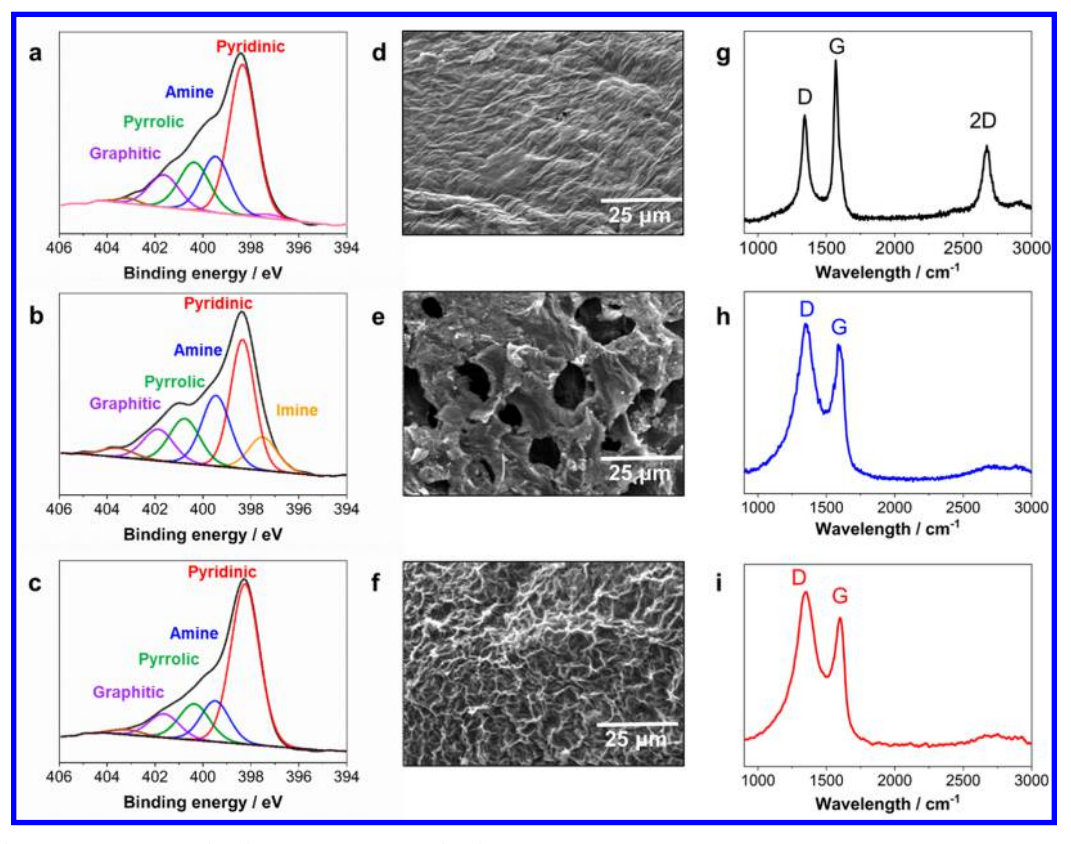


Figure 2. (a-c) XPS N 1s spectra, (d-f) SEM images, and (g-i) Raman spectra of the best performing NrGO catalysts treated with selected solvents including water (a, d, g), diethyl ether (b, e, h), and pyridine (c, f, i).

solvent-treated samples with all catalysts exhibiting a *d*-spacing of 3.4 Å with a broad graphitic peak at 26°, which is indicative of a small crystallite size ⁵³ (Figure S2). XPS data displayed a similar C 1s spectrum (Figure S3), i.e., predominantly graphitic carbon (284.7 eV) with some presence of C-O (286.3 eV) and C=O species (286.3 and 287.8 eV). N 1s spectra shown in Figure 2a-c show the presence of pyridinic, amine, pyrrolic, and graphitic nitrogen (at 398.5, 399.5, and 400.5 eV, respectively). Moreover, diethyl ether- and ethanol-treated samples have slightly higher concentration of nitride edge sites, such as imines or nitriles (397.4 eV), as shown in Figure 2c and Figure S3. The total nitrogen content of all NrGO catalysts varies between 5 and 7 atomic % (Figure S4).

Raman spectroscopy performed on water-, diethyl ether-, and pyridine-treated samples is depicted in Figures 2g, 2h, and 2i, respectively. All spectra show the presence of a peak at 1350 cm⁻¹ corresponding to the D-band, the disorder-induced band, typically seen in graphene-based materials, as well as a peak at 1600 cm⁻¹ corresponding to the G-band, originating from graphite-like sp² hybridization of carbon. Additionally, the water-treated sample (Figure 2g) shows a strong peak at 2670 cm⁻¹ corresponding to the 2D band of graphene or NrGO, whereas the same peak is weakened for the diethyl ether- and pyridine-treated samples. The weakened 2D peak and enhanced D peak for the NrGO obtained from aqueous solvent are specific to few-layered reduced graphene oxide. 54,55 In general, solvent-treated NrGO electrocatalysts have Raman signatures specific to disordered, defected, few-layered graphene, as indicated by a change in the D/G ratio with an increased D-bandwidth and disappearance of the 2D peak. 56

While there were few differences between XRD and XPS spectra among NrGO electrocatalysts, significant morpholog-

ical differences were consistently observed from SEM (Figure 2d-f). The water-treated sample displayed a smooth surface with very few edges exposed or defects and correlates well with the Raman signatures of the samples. The pyridine-treated catalyst showed the roughest surface (largest value of average surface roughness $R_a = 49$ calculated using digital image processing⁵⁷) among all samples (R_a for water and diethyl ether samples are 29 and 38, respectively) with extremely small wrinkles covering the entire surface. The ether-treated catalyst displayed a high concentration of defects in the graphitic lattice between 5 and 20 μ m in diameter ("holey" NrGO). ⁴³ Porosity calculated from the SEM images⁵⁸ shows that the diethyl ethertreated sample has highest porosity of 14-20%, while much smaller porosity was obtained for pyridine- and water-treated samples (4-7% and 1-2%, respectively). The ethanol-treated sample showed a rough and wrinkled surface, exposing edges, as well as a few holes ranging from 2 to 10 μ m in diameter (Figure S5). The porosity and surface roughness can affect the wetting characteristics of the samples, which are crucial for optimizing catalyst for the ORR reaction. Therefore, the impact of these morphological features on the materials wettability was studied using contact angle measurements (Figure S6). The contact angle between water and an NrGO catalyst was measured for the water-, diethyl ether-, and pyridine-treated samples. The contact angles for respective catalyst films were 150°, 50°, and 30°, respectively, indicating that wetting characteristics are enhanced with solvent treatment. Of the three treatments, the one with pyridine appears to allow for a triple-phase boundary (electrolyte, catalyst, and gas phase reactants) ideal for ORR.

The electrocatalytic ORR activity and selectivity of the NrGO electrocatalysts were measured using a rotating ring-

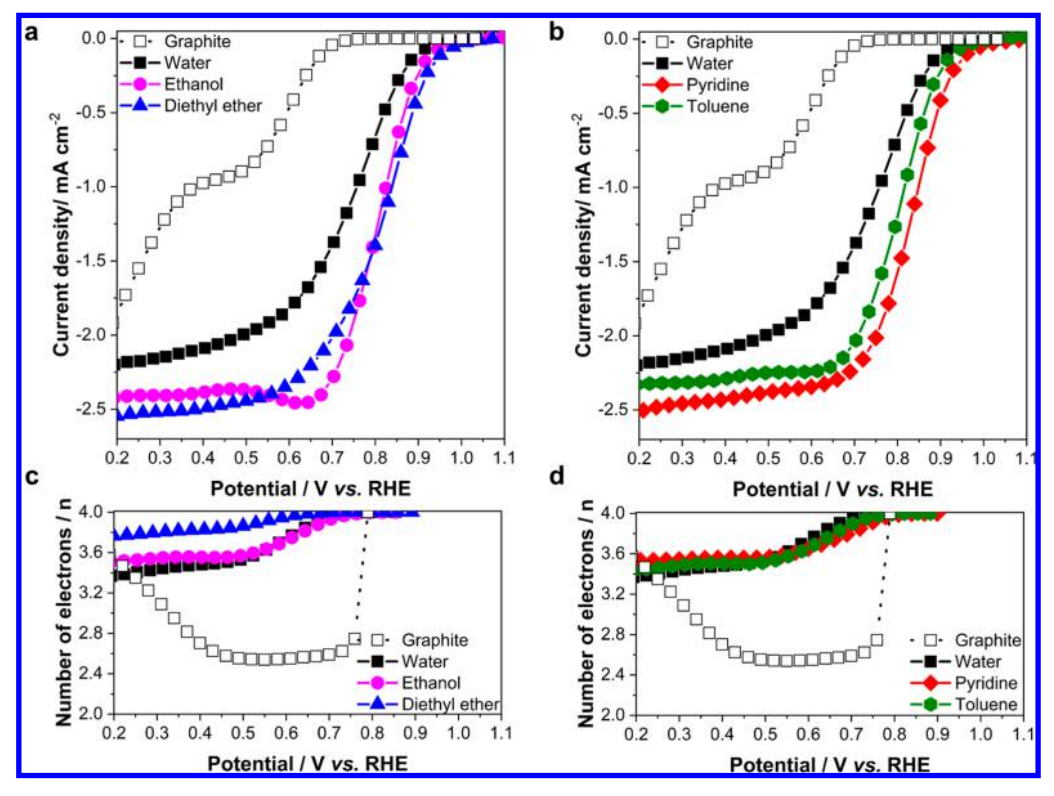


Figure 3. Electrocatalytic activity and selectivity of solvent-treated nitrogen-doped GO catalysts for the oxygen reduction reaction. (a) ORR activity of NrGO catalysts treated with noncyclic solvents. (b) ORR activity of NrGO catalysts treated with cyclic solvents. (c) ORR selectivity of NrGO catalysts treated with noncyclic solvents. (d) ORR selectivity of NrGO catalysts treated with cyclic solvents. NrGO—water data are added for comparison purposes. RRDE conditions: steady-state voltammetry using 30 mV potential step and 30 s potential hold time at every step; Pt ring held at a constant potential of 1.3 V vs RHE; electrolyte 0.1 M NaOH; temperature 25 °C; rotation rate 900 rpm.

disc electrode (RRDE) in O₂-saturated 0.1 M NaOH electrolyte (Figure 3). The number of electrons transferred per molecule of oxygen, i.e., an indicator of the selectivity for the ORR and therefore of the amount of hydroperoxyl radicals generated, was determined according to the following equation:

$$n = 4 \times \frac{i_{\rm d}}{i_{\rm d} + \frac{i_{\rm r}}{N}} \tag{4}$$

where n is the number of transferred electrons transferred per molecule of oxygen, i_d the disc current, i_r the ring current, and N the collection efficiency of the ring. Selectivity toward the four-electron transfer reaction refers to the generation of four OH⁻ according to eq 1. The undesired alternate reaction that could also occur is the partial reduction of O₂ to a HO₂ shown in eq 2. The ORR performance of a catalyst is defined by its high activity and its absence of hydroperoxyl radical generation and, more importantly, by its half-wave potential $(E_{1/2})$ and onset potential (E_{onset}) of the catalyst, i.e., the potential at which the ORR starts to occur. The thermodynamic reversible potential (E°) of the oxygen reduction reaction at 25 °C is 1.23 V versus the reversible hydrogen electrode (RHE). Any additional potential required to drive the ORR is called the overpotential (η). High-performing ORR catalysts are characterized by low η , high $E_{1/2}$, high selectivity values for four-electron transfer and high limiting current. As a reference, graphite shows an $E_{\rm onset}$ of 0.79 V vs RHE with no limiting current and low selectivity for the four-electron reaction (n = 2.5). The observed ORR activity and selectivity for the NrGO electrocatalysts varied depending on the solvent used to treat the graphene oxide precursor prior to N-doping. Lower performance and selectivity were observed from the water-treated NrGO with an E_{onset} of 1.03 V vs RHE and an $E_{1/2}$ of 0.77 V vs RHE. Comparable onset potentials were obtained with other solvents: for noncyclic solvents, ethanoland ether-treated NrGO catalysts demonstrated an Eonset of 1.07 and 1.10 V vs RHE, respectively, whereas cyclic solvents such as pyridine and toluene showed E_{onset} of 1.03 and 1.11 V vs RHE, respectively. In contrast, there was a significant shift toward a more positive $E_{1/2}$, revealing an improvement of the activity and selectivity of the solvent-treated NrGO catalysts. In the case of noncyclic solvents, ethanol- or ether-treated NrGO shifted $E_{1/2}$ to 0.81 V vs RHE. In the case of cyclic solvents, the toluene-treated NrGO shifted $E_{1/2}$ to 0.80 V vs RHE, while the pyridine-treated NrGO exhibited the highest ORR activity with an $E_{1/2}$ of 0.84 V vs RHE. The current generated from the oxidation of HO2 was also recorded during the ORR polarization curves and converted to number of electrons as shown in eq 4. All catalysts showed a combination of 2- and 4-electron reactions, with water showing n = 3.3 at 0.5 V vs RHE. The n values for ethanol-, diethyl ether-, pyridine-, and toluene-treated samples were 3.5, 3.8, 3.5, and 3.4 at 0.5 V vs RHE, respectively. Based on these results, diethyl ether- and pyridine-treated samples showed the highest selectivity and performance in alkaline electrolyte. For comparison, a standard graphite electrode is shown in Figure 3, wherein n = 2.5 is observed. In contrast, platinum reportedly reduces oxygen via a 4-electron (n = 4) transfer reaction.⁵ Therefore, it is evident that solvent-treatment prior to nitrogen doping has a drastic effect on catalytic activity and more importantly leads to an increased number of electrons

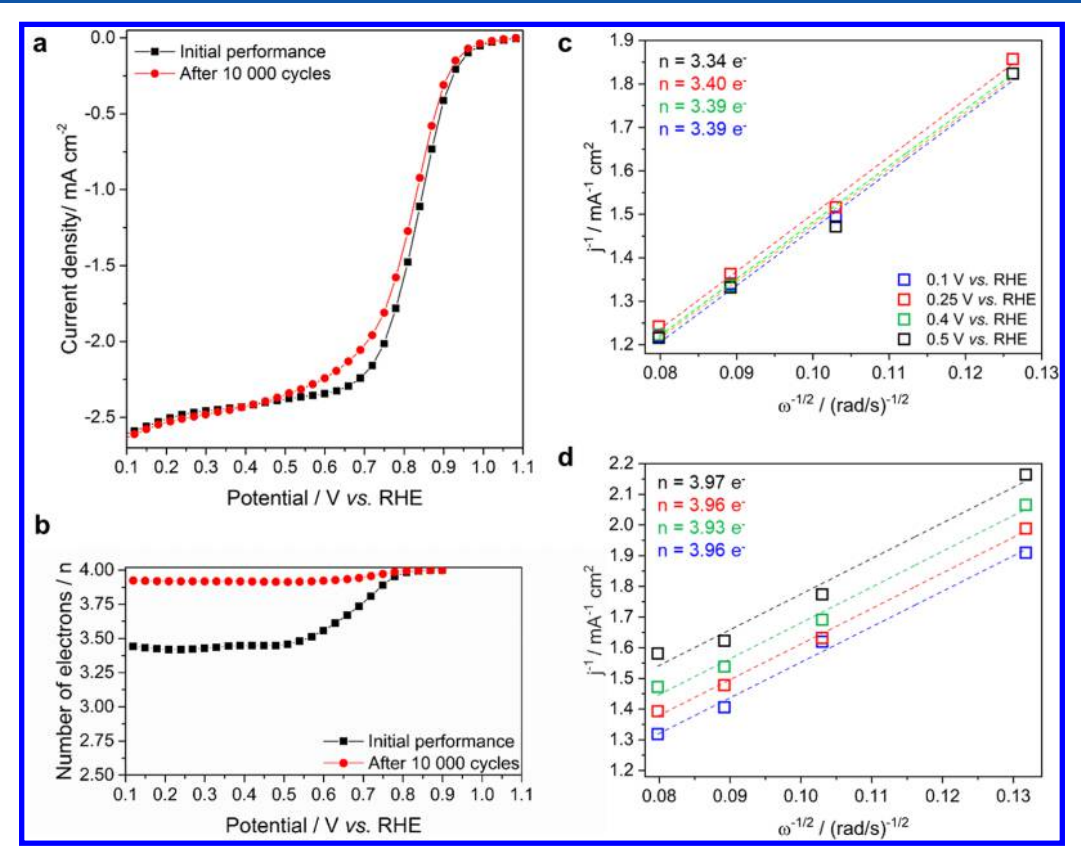


Figure 4. Selectivity, durability, and kinetic activity of NrGO derived from pyridine rinsed GO. (a) RRDE measurement of ORR activity before and after 10000 cycles in N2. (b) Peroxide yield (in terms of number of electrons) before and after 10000 cycles. (c) Koutecky-Levich plot before cycling. (d) Koutecky-Levich plot after cycling. RRDE conditions: steady-state voltammetry using 30 mV potential step and 30 s potential hold time at every step; Pt ring held at a constant potential of 1.3 V vs RHE; electrolyte 0.1 M NaOH; temperature 25 °C; rotation rate 900 rpm.

transferred as indicated by the selectivity data. In fact, according to the previous contact angle measurements and SEM imaging (Figures 2g-i and Figure S5), strongly suggest that the morphology resulting from the solvent treatment, creating the porosity and surface roughness, are the main contributors to the high activity and low hydroperoxyl yield of these materials.

Stability and durability are another important consideration for an ORR catalyst. Such studies were conducted in N₂saturated media by cycling the catalyst 10000 times from 0.6 to 1.0 V at 100 mV/s. Notably, after 10000 cycles, the ORR performance of the most active electrocatalyst (NrGOpyridine) showed only a 20 mV decrease in half-wave potential (Figure 4a) with an improved selectivity of the catalyst from a mixed reaction (n = 3.5) at 0.5 V to a near 4-electron reaction (Figure 4b). The limiting current stayed constant with a value of 2.5 mA cm⁻². To confirm the results observed from RRDE experiments, Koutecky-Levich plots were derived before and after cycling. These results confirm the transition from a mixed reaction to a highly selective 4-electron reaction and therefore to a huge reduction in hydroperoxyl radical generation (Figure 4c,d).

As mentioned previously, the ORR activity shows an initial mixed mechanism of n = 3.4 electrons per molecule of oxygen. This initial performance is the combination of different active sites, promoting either a 2- or a 4-electron reaction. As we cycle the catalyst in a reductive environment, the mechanism shifts toward a more selective 4-electron process despite a minimal half-wave potential decrease and no limiting current change (Figure 4). This data suggests that the reduction of oxygen initially occurs via two 2-electron reaction. Furthermore, the question arises that the cycling of the electrocatalysts either destroys sites promoting the first reaction leading to peroxide radicals being formed, as shown in eq 2, or unveils more active sites dedicated to the reduction of peroxide radicals into hydroxides shown in eq 3. To understand by which mechanism higher selectivity is achieved, chronoamperometry was performed in the presence of peroxide in the electrolyte. The reduction of these radicals into OH by the catalysts is shown in Figure S7 and clearly indicates that a reduction current appearing as 1 mmol of peroxide radicals is being introduced in the solution. Additionally, there is no change in current density or in slope before and after cycling. This suggests that the rate of decomposition of peroxide radicals remains the same and therefore that cycling the catalyst would destroy peroxide-generating active sites (eq 2) rather than unveiling new peroxide-reducing active sites. Understanding the mechanism of selectivity of iron-free, carbon-based, PGM-free catalysts for ORR relies on their chemical moieties, their surface concentration, and their morphology through accessibility to the active sites. The treatment of this work in 2D materials is hindered by the low active site surface concentration, while moving to 3D structure made of 2D materials (this work), the challenge lays primarily in the control of morphology. The morphology of M-N-C catalysts is as complex as or even more complex than the model catalyst described in this work. The critical attempt made here is to reveal that the synthetic path which involves solvent, facilitating the stacking of these graphene materials, is a major contributor to morphology. In fact, as mentioned in a

previous study,⁴³ the solvents leading to the best performing NrGO catalysts, namely diethyl ether and pyridine, can presumably substantially alter the structure of water-intercalated GO. This is likely due upon annealing to (i) confined water molecules that could form holes perpendicular to the sheets as they escape in the case of diethyl ether 52,59 or (ii) a reduced d-spacing between GO sheets as solvents are escaping as seen in the case of ethanol and pyridine. 51,59 The role of graphene stacking in M-N-C catalysts was linked to the nature of the actives sites as in-plane or edge defect. 60 For platinum catalysts, morphology and activity interplay dramatically depends on carbon support structure, and it becomes even more important with transition toward low-PGM catalysts.61-63 In the presented work, the concentration of active sites appears to be directly related to the morphology of the material, through either in-plane roughness or the creation of holes, associated with a high concentration of edges. In GO and NrGO, the oxygen-containing groups are usually associated with edge defect. With ORR following a 2 + 2electron reaction mechanism, it is likely that the second 2electron reaction involving the reduction of HO₂⁻ groups to OH⁻ directly involve oxygen-containing edges.

In summary, we have shown that exposing our model catalyst, GO, to various solvent treatments results in electrocatalysts with very different morphology after nitrogen doping in an ammonia environment at 850 °C. These resulting morphological differences lead to materials with different ORR selectivity exhibiting both 2 + 2- and 4-electron catalytic behavior. However, after cycling the NrGO electrocatalyst rinsed in pyridine in an RRDE experiment, we found that the material shifted its ORR behavior to a predominantly 4electron reaction, i.e., its generation of hydroperoxyl radicals, detrimental to fuel cell durability, dropped significantly, with little loss in overall performance. The cycling of the catalysts destroys active sites promoting the reduction of oxygen to peroxide radicals. Because this observation was only found in an alkaline medium (similar experiments in acid showed no selectivity changes⁴³), this suggests that the active sites in acid and alkaline are likely different and that electrocatalysts should each be tailored depending on the application. Finally, the treatment of other existing PGM-free systems with organic solvents could introduce morphological changes that could lead to more active, more selective, and more durable catalysts for ORR.

ASSOCIATED CONTENT

S Supporting Information

The Supporting Information is available free of charge on the ACS Publications website at DOI: 10.1021/acsanm.8b02235.

Experimental procedures, X-ray diffraction patterns, XPS spectra, scanning electron microscopy images, chronoamperometry experiments (PDF)

AUTHOR INFORMATION

Corresponding Author

*E-mail: gautam.gupta@louisville.edu.

ORCID ®

Joseph H. Dumont: 0000-0001-9698-0995 Ulises Martinez: 0000-0001-8239-0281 Kateryna Artyushkova: 0000-0002-2611-0422 Aditya Mohite: 0000-0001-8865-409X

Plamen Atanassov: 0000-0003-2996-472X

Present Address

G.G.: Chemical Engineering, University of Louisville, Louisville, KY 40292.

Notes

The authors declare no competing financial interest.

ACKNOWLEDGMENTS

The authors thank the Los Alamos National Laboratory for funding this research through the Laboratory Directed Research and Development (LDRD) program, Award 20130065DR. This material is based upon work supported by the National Science Foundation under Grant 1800245.

REFERENCES

- (1) Hou, J.; Shao, Y.; Ellis, M. W.; Moore, R. B.; Yi, B. Graphene-Based Electrochemical Energy Conversion and Storage: Fuel Cells, Supercapacitors and Lithium Ion Batteries. Phys. Chem. Chem. Phys. **2011**, 13 (34), 15384–15402.
- (2) Pumera, M. Graphene-Based Nanomaterials for Energy Storage. Energy Environ. Sci. 2011, 4 (3), 668-674.
- (3) Bonaccorso, F.; Colombo, L.; Yu, G.; Stoller, M.; Tozzini, V.; Ferrari, A. C.; Ruoff, R. S.; Pellegrini, V. Graphene, Related Two-Dimensional Crystals, and Hybrid Systems for Energy Conversion and Storage. Science 2015, 347 (6217), 1246501.
- (4) Raccichini, R.; Varzi, A.; Passerini, S.; Scrosati, B. The Role of Graphene for Electrochemical Energy Storage. Nat. Mater. 2015, 14 (3), 271-279.
- (5) Geniès, L.; Faure, R.; Durand, R. Electrochemical Reduction of Oxygen on Platinum Nanoparticles in Alkaline Media. Electrochim. Acta 1998, 44 (8-9), 1317-1327.
- (6) Gasteiger, H. A.; Kocha, S. S.; Sompalli, B.; Wagner, F. T. Activity Benchmarks and Requirements for Pt, Pt-Alloy, and Non-Pt Oxygen Reduction Catalysts for Pemfcs. Appl. Catal., B 2005, 56 (1), 9-35.
- (7) Gong, K.; Du, F.; Xia, Z.; Durstock, M.; Dai, L. Nitrogen-Doped Carbon Nanotube Arrays with High Electrocatalytic Activity for Oxygen Reduction. Science 2009, 323 (5915), 760-764.
- (8) Liang, Y.; Li, Y.; Wang, H.; Zhou, J.; Wang, J.; Regier, T.; Dai, H. Co3o4 Nanocrystals on Graphene as a Synergistic Catalyst for Oxygen Reduction Reaction. Nat. Mater. 2011, 10 (10), 780-786.
- (9) Merle, G.; Wessling, M.; Nijmeijer, K. Anion Exchange Membranes for Alkaline Fuel Cells: A Review. J. Membr. Sci. 2011, 377 (1), 1-35.
- (10) Varcoe, J. R.; Slade, R. C. Prospects for Alkaline Anion-Exchange Membranes in Low Temperature Fuel Cells. Fuel Cells **2005**, 5 (2), 187–200.
- (11) Kinumoto, T.; Inaba, M.; Nakayama, Y.; Ogata, K.; Umebayashi, R.; Tasaka, A.; Iriyama, Y.; Abe, T.; Ogumi, Z. Durability of Perfluorinated Ionomer Membrane against Hydrogen Peroxide. J. Power Sources 2006, 158 (2), 1222-1228.
- (12) Wilson, M. S.; Gottesfeld, S. Thin-Film Catalyst Layers for Polymer Electrolyte Fuel Cell Electrodes. J. Appl. Electrochem. 1992, 22 (1), 1-7.
- (13) Wang, B. Recent Development of Non-Platinum Catalysts for Oxygen Reduction Reaction. J. Power Sources 2005, 152, 1-15.
- (14) Bashyam, R.; Zelenay, P. A Class of Non-Precious Metal Composite Catalysts for Fuel Cells. Nature 2006, 443 (7107), 63-66. (15) Jaouen, F.; Herranz, J.; Lefevre, M.; Dodelet, J.-P.; Kramm, U. I.; Herrmann, I.; Bogdanoff, P.; Maruyama, J.; Nagaoka, T.; Garsuch, A.; et al. Cross-Laboratory Experimental Study of Non-Noble-Metal Electrocatalysts for the Oxygen Reduction Reaction. ACS Appl. Mater. Interfaces 2009, 1 (8), 1623-1639.
- (16) Chung, H. T.; Johnston, C. M.; Artyushkova, K.; Ferrandon, M.; Myers, D. J.; Zelenay, P. Cyanamide-Derived Non-Precious Metal Catalyst for Oxygen Reduction. Electrochem. Commun. 2010, 12 (12), 1792-1795.

- (17) Garsuch, A.; Bonakdarpour, A.; Liu, G.; Yang, R.; Dahn, J. R. Time to Move Beyond Transition Metal-N-C Catalysts for Oxygen Reduction. In *Handbook of Fuel Cells*; John Wiley & Sons, Ltd.: 2010.
- (18) Jaouen, F.; Proietti, E.; Lefèvre, M.; Chenitz, R.; Dodelet, J.-P.; Wu, G.; Chung, H. T.; Johnston, C. M.; Zelenay, P. Recent Advances in Non-Precious Metal Catalysis for Oxygen-Reduction Reaction in Polymer Electrolyte Fuel Cells. *Energy Environ. Sci.* **2011**, *4* (1), 114–130.
- (19) Proietti, E.; Jaouen, F.; Lefèvre, M.; Larouche, N.; Tian, J.; Herranz, J.; Dodelet, J.-P. Iron-Based Cathode Catalyst with Enhanced Power Density in Polymer Electrolyte Membrane Fuel Cells. *Nat. Commun.* **2011**, *2*, 416.
- (20) Wu, G.; Johnston, C. M.; Mack, N. H.; Artyushkova, K.; Ferrandon, M.; Nelson, M.; Lezama-Pacheco, J. S.; Conradson, S. D.; More, K. L.; Myers, D. J.; Zelenay, P. Synthesis—Structure—Performance Correlation for Polyaniline—Me—C Non-Precious Metal Cathode Catalysts for Oxygen Reduction in Fuel Cells. *J. Mater. Chem.* **2011**, 21 (30), 11392—11405.
- (21) Wu, G.; More, K. L.; Johnston, C. M.; Zelenay, P. High-Performance Electrocatalysts for Oxygen Reduction Derived from Polyaniline, Iron, and Cobalt. *Science* **2011**, 332 (6028), 443–447.
- (22) Serov, A.; Robson, M. H.; Artyushkova, K.; Atanassov, P. Templated Non-Pgm Cathode Catalysts Derived from Iron and Poly (Ethyleneimine) Precursors. *Appl. Catal., B* **2012**, *127*, 300–306.
- (23) Serov, A.; Robson, M. H.; Halevi, B.; Artyushkova, K.; Atanassov, P. Highly Active and Durable Templated Non-Pgm Cathode Catalysts Derived from Iron and Aminoantipyrine. *Electro-chem. Commun.* **2012**, 22, 53–56.
- (24) Lee, J.-S.; Park, G. S.; Kim, S. T.; Liu, M.; Cho, J. A Highly Efficient Electrocatalyst for the Oxygen Reduction Reaction: N-Doped Ketjenblack Incorporated into Fe/Fe3c-Functionalized Melamine Foam. *Angew. Chem., Int. Ed.* **2013**, *52* (3), 1026–1030.
- (25) Ranjbar Sahraie, N.; Paraknowitsch, J. P.; Göbel, C.; Thomas, A.; Strasser, P. Noble-Metal-Free Electrocatalysts with Enhanced Orr Performance by Task-Specific Functionalization of Carbon Using Ionic Liquid Precursor Systems. *J. Am. Chem. Soc.* **2014**, *136* (41), 14486–14497.
- (26) Tylus, U.; Jia, Q.; Strickland, K.; Ramaswamy, N.; Serov, A.; Atanassov, P.; Mukerjee, S. Elucidating Oxygen Reduction Active Sites in Pyrolyzed Metal—Nitrogen Coordinated Non-Precious-Metal Electrocatalyst Systems. *J. Phys. Chem. C* **2014**, *118* (17), 8999—9008.
- (27) Gupta, S.; Tryk, D.; Bae, I.; Aldred, W.; Yeager, E. Heat-Treated Polyacrylonitrile-Based Catalysts for Oxygen Electroreduction. *J. Appl. Electrochem.* **1989**, *19* (1), 19–27.
- (28) Lalande, G.; Cote, R.; Guay, D.; Dodelet, J.; Weng, L.; Bertrand, P. Is Nitrogen Important in the Formulation of Fe-Based Catalysts for Oxygen Reduction in Solid Polymer Fuel Cells? *Electrochim. Acta* 1997, 42 (9), 1379–1388.
- (29) Kobayashi, M.; Niwa, H.; Harada, Y.; Horiba, K.; Oshima, M.; Ofuchi, H.; Terakura, K.; Ikeda, T.; Koshigoe, Y.; Ozaki, J.-i.; Miyata, S.; Ueda, S.; Yamashita, Y.; Yoshikawa, H.; Kobayashi, K. Role of Residual Transition-Metal Atoms in Oxygen Reduction Reaction in Cobalt Phthalocyanine-Based Carbon Cathode Catalysts for Polymer Electrolyte Fuel Cell. *J. Power Sources* **2011**, *196* (20), 8346–8351.
- (30) Kobayashi, M.; Niwa, H.; Saito, M.; Harada, Y.; Oshima, M.; Ofuchi, H.; Terakura, K.; Ikeda, T.; Koshigoe, Y.; Ozaki, J.-i.; Miyata, S. Indirect Contribution of Transition Metal Towards Oxygen Reduction Reaction Activity in Iron Phthalocyanine-Based Carbon Catalysts for Polymer Electrolyte Fuel Cells. *Electrochim. Acta* 2012, 74, 254–259.
- (31) Marcano, D. C.; Kosynkin, D. V.; Berlin, J. M.; Sinitskii, A.; Sun, Z.; Slesarev, A.; Alemany, L. B.; Lu, W.; Tour, J. M. Improved Synthesis of Graphene Oxide. *ACS Nano* **2010**, *4* (8), 4806–4814.
- (32) Hummers, W. S.; Offeman, R. E. Preparation of Graphitic Oxide. J. Am. Chem. Soc. 1958, 80 (6), 1339–1339.
- (33) Dreyer, D. R.; Park, S.; Bielawski, C. W.; Ruoff, R. S. The Chemistry of Graphene Oxide. *Chem. Soc. Rev.* **2010**, 39 (1), 228–240.

- (34) Dimiev, A.; Kosynkin, D. V.; Alemany, L. B.; Chaguine, P.; Tour, J. M. Pristine Graphite Oxide. *J. Am. Chem. Soc.* **2012**, *134* (5), 2815–2822.
- (35) Jia, Q.; Ramaswamy, N.; Tylus, U.; Strickland, K.; Li, J.; Serov, A.; Artyushkova, K.; Atanassov, P.; Anibal, J.; Gumeci, C.; Barton, S. C.; Sougrati, M.-T.; Jaouen, F.; Halevi, B.; Mukerjee, S. Spectroscopic Insights into the Nature of Active Sites in Iron—Nitrogen—Carbon Electrocatalysts for Oxygen Reduction in Acid. *Nano Energy* **2016**, *29*, 65–82.
- (36) Geng, D.; Chen, Y.; Chen, Y.; Li, Y.; Li, R.; Sun, X.; Ye, S.; Knights, S. High Oxygen-Reduction Activity and Durability of Nitrogen-Doped Graphene. *Energy Environ. Sci.* **2011**, *4* (3), 760–764
- (37) Jafri, R. I.; Rajalakshmi, N.; Ramaprabhu, S. Nitrogen Doped Graphene Nanoplatelets as Catalyst Support for Oxygen Reduction Reaction in Proton Exchange Membrane Fuel Cell. *J. Mater. Chem.* **2010**, 20 (34), 7114–7117.
- (38) Lee, K. R.; Lee, K. U.; Lee, J. W.; Ahn, B. T.; Woo, S. I. Electrochemical Oxygen Reduction on Nitrogen Doped Graphene Sheets in Acid Media. *Electrochem. Commun.* **2010**, *12* (8), 1052–1055
- (39) Ozaki, J.-i.; Kimura, N.; Anahara, T.; Oya, A. Preparation and Oxygen Reduction Activity of Bn-Doped Carbons. *Carbon* **2007**, *45* (9), 1847–1853.
- (40) Qu, L.; Liu, Y.; Baek, J.-B.; Dai, L. Nitrogen-Doped Graphene as Efficient Metal-Free Electrocatalyst for Oxygen Reduction in Fuel Cells. *ACS Nano* **2010**, *4* (3), 1321–1326.
- (41) Shao, Y.; Zhang, S.; Engelhard, M. H.; Li, G.; Shao, G.; Wang, Y.; Liu, J.; Aksay, I. A.; Lin, Y. Nitrogen-Doped Graphene and Its Electrochemical Applications. *J. Mater. Chem.* **2010**, 20 (35), 7491–7496.
- (42) Sheng, Z.-H.; Shao, L.; Chen, J.-J.; Bao, W.-J.; Wang, F.-B.; Xia, X.-H. Catalyst-Free Synthesis of Nitrogen-Doped Graphene Via Thermal Annealing Graphite Oxide with Melamine and Its Excellent Electrocatalysis. *ACS Nano* **2011**, *5* (6), 4350–4358.
- (43) Martinez, U.; Dumont, J. H.; Holby, E. F.; Artyushkova, K.; Purdy, G. M.; Singh, A.; Mack, N. H.; Atanassov, P.; Cullen, D. A.; More, K. L.; Chhowalla, M.; Zelenay, P.; Dattelbaum, A. M.; Mohite, A. D.; Gupta, G. Critical Role of Intercalated Water for Electrocatalytically Active Nitrogen-Doped Graphitic Systems. *Sci. Adv.* 2016, DOI: 10.1126/sciadv.1501178.
- (44) Wei, W.; Liang, H.; Parvez, K.; Zhuang, X.; Feng, X.; Müllen, K. Nitrogen-Doped Carbon Nanosheets with Size-Defined Mesopores as Highly Efficient Metal-Free Catalyst for the Oxygen Reduction Reaction. *Angew. Chem., Int. Ed.* **2014**, *53* (6), 1570–1574.
- (45) Bikkarolla, S. K.; Cumpson, P.; Joseph, P.; Papakonstantinou, P. Oxygen Reduction Reaction by Electrochemically Reduced Graphene Oxide. *Faraday Discuss.* **2014**, *173* (0), 415–428.
- (46) Lai, L.; Potts, J. R.; Zhan, D.; Wang, L.; Poh, C. K.; Tang, C.; Gong, H.; Shen, Z.; Lin, J.; Ruoff, R. S. Exploration of the Active Center Structure of Nitrogen-Doped Graphene-Based Catalysts for Oxygen Reduction Reaction. *Energy Environ. Sci.* **2012**, 5 (7), 7936–7942.
- (47) Artyushkova, K.; Serov, A.; Rojas-Carbonell, S.; Atanassov, P. Chemistry of Multitudinous Active Sites for Oxygen Reduction Reaction in Transition Metal—Nitrogen—Carbon Electrocatalysts. *J. Phys. Chem. C* **2015**, *119* (46), 25917—25928.
- (48) Zitolo, A.; Goellner, V.; Armel, V.; Sougrati, M.-T.; Mineva, T.; Stievano, L.; Fonda, E.; Jaouen, F. Identification of Catalytic Sites for Oxygen Reduction in Iron- and Nitrogen-Doped Graphene materials. *Nat. Mater.* **2015**, *14*, 937.
- (49) Strickland, K.; Miner, E.; Jia, Q.; Tylus, U.; Ramaswamy, N.; Liang, W.; Sougrati, M.-T.; Jaouen, F.; Mukerjee, S. Highly Active Oxygen Reduction Non-Platinum Group Metal Electrocatalyst without Direct Metal—Nitrogen Coordination. *Nat. Commun.* **2015**, 6, 7343.
- (50) Kabir, S.; Artyushkova, K.; Serov, A.; Atanassov, P. Role of Nitrogen Moieties in N-Doped 3d-Graphene Nanosheets for Oxygen

- Electroreduction in Acidic and Alkaline Media. ACS Appl. Mater. Interfaces 2018, 10 (14), 11623–11632.
- (51) Paredes, J.; Villar-Rodil, S.; Martínez-Alonso, A.; Tascon, J. Graphene Oxide Dispersions in Organic Solvents. *Langmuir* **2008**, 24 (19), 10560–10564.
- (52) Park, S.; An, J.; Jung, I.; Piner, R. D.; An, S. J.; Li, X.; Velamakanni, A.; Ruoff, R. S. Colloidal Suspensions of Highly Reduced Graphene Oxide in a Wide Variety of Organic Solvents. *Nano Lett.* **2009**, 9 (4), 1593–1597.
- (53) Some, S.; Kim, Y.; Yoon, Y.; Yoo, H.; Lee, S.; Park, Y.; Lee, H. High-Quality Reduced Graphene Oxide by a Dual-Function Chemical Reduction and Healing Process. *Sci. Rep.* **2013**, *3*, 1929.
- (54) Zhao, W.; Tan, P. H.; Liu, J.; Ferrari, A. C. Intercalation of Few-Layer Graphite Flakes with Fecl3: Raman Determination of Fermi Level, Layer by Layer Decoupling, and Stability. *J. Am. Chem. Soc.* **2011**, *133* (15), 5941–5946.
- (55) Yang, H.; Hu, H.; Ni, Z.; Poh, C. K.; Cong, C.; Lin, J.; Yu, T. Comparison of Surface-Enhanced Raman Scattering on Graphene Oxide, Reduced Graphene Oxide and Graphene Surfaces. *Carbon* **2013**, *62* (Suppl.C), 422–429.
- (56) Kaniyoor, A.; Ramaprabhu, S. A Raman Spectroscopic Investigation of Graphite Oxide Derived Graphene. *AIP Adv.* **2012**, 2 (3), No. 032183.
- (57) Artyushkova, K.; Fulghum, J. E. Angle Resolved Imaging of Polymer Blend Systems: From Images to a 3d Volume of Material Morphology. J. Electron Spectrosc. Relat. Phenom. 2005, 149 (1–3), 51–60.
- (58) Artyushkova, K.; Pylypenko, S.; Dowlapalli, M.; Atanassov, P. Use of Digital Image Processing of Microscopic Images and Multivariate Analysis for Quantitative Correlation of Morphology, Activity and Durability of Electrocatalysts. *RSC Adv.* **2012**, *2* (10), 4304–4310.
- (59) Martinez, U.; Dumont, J. H.; Holby, E. F.; Artyushkova, K.; Purdy, G. M.; Singh, A.; Mack, N. H.; Atanassov, P.; Cullen, D. A.; More, K. L.; et al. Critical Role of Intercalated Water for Electrocatalytically Active Nitrogen-Doped Graphitic Systems. *Science advances* **2016**, 2 (3), No. e1501178.
- (60) Workman, M. J.; Serov, A.; Tsui, L.-k.; Atanassov, P.; Artyushkova, K. Fe-N-C Catalyst Graphitic Layer Structure and Fuel Cell Performance. ACS Energy Letters 2017, 2 (7), 1489–1493.
- (61) Yarlagadda, V.; Carpenter, M. K.; Moylan, T. E.; Kukreja, R. S.; Koestner, R.; Gu, W.; Thompson, L.; Kongkanand, A. Boosting Fuel Cell Performance with Accessible Carbon Mesopores. *ACS Energy Letters* **2018**, *3* (3), 618–621.
- (62) Watanabe, M.; Tryk, D. A. The Role of Carbon Blacks as Catalyst Supports and Structural Elements in Polymer Electrolyte Fuel Cells. In *Nanocarbons for Energy Conversion: Supramolecular Approaches*; Springer: 2019; pp 81–118.
- (63) Kongkanand, A.; Mathias, M. F. The Priority and Challenge of High-Power Performance of Low-Platinum Proton-Exchange Membrane Fuel Cells. *J. Phys. Chem. Lett.* **2016**, *7* (7), 1127–1137.